Connectionism in Perspective,
(North-Holland, Amsterdam, 1989)
pp.403-412

Kohonen's Self-organizing Map for Modeling the Formation of the Auditory Cortex of a Bat

Thomas Martinetz, Helge Ritter and Klaus Schulten
Department of Physics
Technical University of Munich
D-8046 Garching

Abstract: As an example of Kohonen's self-organizing mapping algorithm we simulate the formation of a disproportionate representation of the ultrasound spectrum by the auditory cortex of a bat. We compare the results with experimental data of the cortex of the mustache bat *Pteronotus parnelli rubiginosus* and with an analytical calculation.

1. Introduction

A most important task for the brain is a good representation of its sensory data. In the early stages of sensory processing , this is achieved by connecting cortical neurons to their peripheral receptors in a topology conserving fashion. In this way, neighbouring neurons in the cortex can get tuned to similar sensory inputs. The extent of cortical representations of peripheral sensory fields is greatly varying, depending on the functional importance of the sensory signals for the species behaviour. Within the cortex, the size of the population of neurons concerned with particular sensory signals depends also on the fine analysis necessary for these signals. For example, the fine analysis of visual information in higher mammals is mainly performed at the *fovea centralis.* The *fovea centralis* is a very small area near the center of the retina with a high density of sensory cells. Therefore, the resolution in this area is much higher than in the areas of the retina which are responsible for the periphery of the visual field. Although the *fovea centralis* is much smaller than the whole retina, it is represented by the largest part of the visual cortex. Similar disproportionate representations were found in the somatosensory system and the motor cortex. For instance, "hand" areas in the somatosensory and motor cortices of monkeys are of considerably larger relative size than the representation of the remainder of the body surface (Woolsey 1958).

In the auditive cortex of mammals, however, a comparably disproportionate projection has not been found. This is probably due to the fact that the acoustic signals used by most mammals have a broad frequency range and their sound energy is commonly not concentrated at any particular frequency. The cry of a cat, for example, contains many harmonics of the principal mode, and no part of the frequency band is more important for survival than the rest. The auditive cortex of cats has been investigated very carefully, and the experiments have indicated, as expected, a nearly proportionate tonotopic representation, without any particular preference to special frequencies. Thereby high-frequency-sensitive neurons have been located on the anterior and low-frequency-sensitive neurons on the posterior part of the cortex, with neurons sensitive to intermediate frequencies lying in between. Analogous, previous investigations show a very similar structure also for the auditive cortex of dogs and monkeys (Merzenich et al. 1975).

2. The auditory cortex of a bat

A completely different case was found, when the auditory cortex of the mustache bat *Pteronotus parnelli rubiginosus* from Panama was investigated. Because of the emitted orientation signals, the frequency spectrum contains some very important parts for the mustache bat. For orientation, it has several location signals at different frequencies to measure the distances of objects in its surroundings by the time delay of the echo. In addition, the mustache bat *Pteronotus parnelli rubiginosus* uses a very intense orientation sound at 61 kHz to determine the velocity of objects by measuring the Doppler shift of the echo. A separate area of the auditory cortex is involved to analyse this Doppler shift. With this area, *Pteronotus parnelli rubiginosus* is able to determine the velocity of enemies and insects, its main food source, to a precision up to 3 cm/s (Suga and Jen 1976).

The Doppler shift of the echo, caused by an object moving in the direction of flight of the bat, is given by (see e.g. Gerthsen et al. 1986)

$$\frac{\Delta f}{f_e} = \frac{2v_{bat}}{c} - \frac{v_{obj}}{c}. \tag{1}$$

f_e denotes the echolocation signal frequency of 61 kHz, v_{bat} the velocity of the bat, v_{obj} the velocity of the detected object and c the speed of sound. In the formula, the velocity of the bat has to be multiplied by a factor of two because of a Doppler shift during the emission of the orientation signal and an additional shift of the same amount during the reception of the echo. An additional frequency shift of v_{obj}/c is caused by the motion of the detected object. If the bat knows its own velocity, it is able to determine v_{obj} by means of the total Doppler shift Δf.

The excellent sonar abilities of the bat are certainly essential for its survival. But to be able to determine a frequency shift of 0.01%, which corresponds approximatly to the velocity of 3 cm/s mentioned above, a particulary high resolution of the echo near the frequency of the orientation signal is necessary. Therefore, it would not be surprising, if the interval of the frequency band around the 61 kHz of the echolocation signal is disproportionally represented at this part of the auditive cortex responsible for the analysis of the Doppler shift. Corresponding investigations at the auditive cortex of *Pteronotus parnelli rubiginosus* have been made and confirm this consideration.

Figure 1 shows the measurements of Suga and Jen (1976). In part B of Fig. 1 we see that the one-dimensional frequency band extends continuously and monotonically mainly along the anteroposterior axis. Furthermore, we can recognize the particularly highly resolved interval around the echolocation frequency of 61 kHz. To emphasize this extreme disproportionality, the shaded region of Fig. 1A is shown separately in Fig. 1C. The region of the cortex drawn shaded in Fig. 1A is associated with that part of the whole frequency band, which is relevant for the orientation of the bat. The "best frequencies" of the neurons in this region extend from their minimum of 20 kHz over the echolocation frequency to their maximum of 100 kHz (the "best frequency" of a neuron is the frequency, which causes its highest excitation). In C, these best frequencies are plotted versus their location on the anteroposterior axis. We see, that an exceptionally large fraction of all neurons is tuned to a very small interval centered around

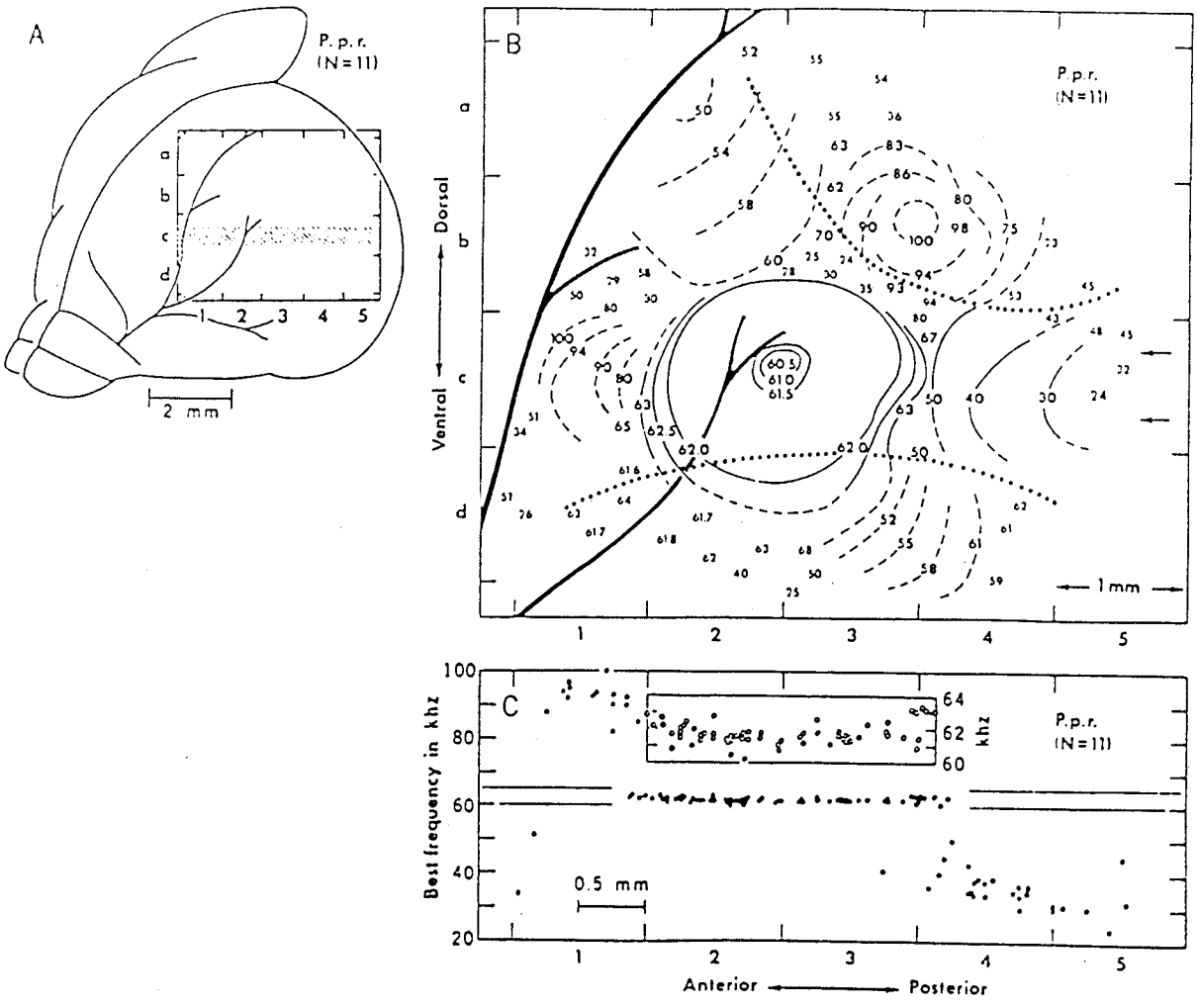

Fig.1 (A) Dorsolateral view of the cerebrum of the mustache bat *Pteronotus parnelli rubiginosus*. The auditory cortices lie inside the rectangle. (B) Distribution of best frequencies in the rectangle shown in (A). The area between the dotted lines is the primary auditory cortex (AI). The areas dorsal or ventral to AI are nonprimary auditory cortices. Orderly tonotopic representation is encountered in the areas with solid contour lines but it is more vague in the areas with dashed contour lines. In the areas where contour lines are not drawn, the tonotopic representation, if present, is obscure. Some of the best frequencies obtained in these areas are shown by small letters. (C) Distribution of the best frequencies along the anteroposterior axis in the shaded area in (A). Since the minor differences among the best frequencies in areas 2 and 3 cannot clearly be shown in (C), the distribution of the best frequencies in this area is shown by the inset with a larger frequency scale and using open circles (from Suga and Jen 1976), (P.p.r., Pteronotus parnelli rubiginosus).

the echolocation frequency. Nearly half of this fraction of the auditory cortex is involved in the analysis of the Doppler shifted echos. This is consistent with the particularly high resolution of 0.01%, enabling the bat to orientate itself in its surroundings and to detect even the wingbeat of small insects.

3. The Model

We want to model the formation of the mapping from the ultrasound spectrum, received by the mustache bat, to the auditive cortex. Several algorithms for the formation of such mappings have been suggested (Edelman 1985; Takeuchi 1979; Willshaw 1976, 1979). In the following we will consider a proposal due to Kohonen (Kohonen 1982a, 1982c, 1984). This proposal does not model biological details but captures the most essential features of such mappings. The aim is to generate a mapping of a space V of input signals onto an discrete lattice A of formal neurons. The map is generated by establishing a correspondence between inputs from V and neurons in the lattice such, that the topological (neighborhood) relationships among the inputs are reflected as faithfully as possible in the arrangement of the corresponding neurons in the lattice. The correspondence is obtained iteratively by a sequence of training steps, which can be formulated in terms of synaptic modification laws (Kohonen 1984) for the neurons. However, for the purposes of this paper, we present the algorithm in an abstract form without explicit reference to neurons.

Each input signal is represented by a vector $\mathbf{f} \in V$. In our special case, $\mathbf{f}$ specifies the frequency of the received ultrasound signals and therefore is one-dimensional. For each training step an input $\mathbf{f} \in V$ is chosen randomly according to some probability of occurrence $P(\mathbf{f})$. Each location $\mathbf{r}$ of the lattice A carries also a vector $\mathbf{w_r} \in V$, in our application the best frequency of neuron $\mathbf{r}$. The vectors $\mathbf{w_r}$ map lattice locations $\mathbf{r}$ to points in V. In our simulation, the $\mathbf{w_r}$ are chosen randomly for the initial state of the mapping, and for each training step this mapping is adjusted by the following two steps:

1. Determine lattice location $\mathbf{s}$ for which

$$||\mathbf{w_s} - \mathbf{f}|| = \min_{\mathbf{r} \in A} ||\mathbf{w_r} - \mathbf{f}|| \tag{2}$$

   where $\mathbf{f}$ is the randomly chosen input signal for the current step.

2. For all sites $\mathbf{r}$ in the neighborhood of $\mathbf{s}$ (with $\mathbf{s}$ included) adjust

$$\mathbf{w_r}^{(new)} = \mathbf{w_r}^{(old)} + \epsilon h_{\mathbf{rs}}(\mathbf{f} - \mathbf{w_r}^{(old)}), \tag{3}$$

   where $0 \leq h_{\mathbf{rs}} \leq 1$ is a prespecified adjustment function of the distance $||\mathbf{r} - \mathbf{s}||$ and ϵ is a learning step size. $h_{\mathbf{rs}}$ has its maximum at $\mathbf{r} = \mathbf{s}$ and usually decays to zero, as $||\mathbf{r} - \mathbf{s}||$ increases.

By decreasing the step size ϵ and the lateral width σ of $h_{\mathbf{rs}}$ slowly with increasing number of training steps, the algorithm can be shown to gradually yield values for the vectors $\mathbf{w_r}$ which define a (discretized) neighborhood conserving mapping between lattice sites $\mathbf{r}$ and points of the input space V (Kohonen, op.cit.).

The formation of the map is driven by a random sequence of sensory input signals whose probability distribution imprints on the final map in such a way that regions of the input signal space corresponding to frequent signal occurences are mapped onto larger areas than regions corresponding to rarer input signals. In our example the input space $P(f)$ is the one-dimensional ultrasound spectrum of the bat. We model this spectrum by superimposing the spectra of white noise of a small amplitude and a gaussian distribution

peaked at 61 kHz. The white noise in the frequency interval between 20 and 100 kHz describes signals of external ultrasound sources. The gaussian distribution at 61 kHz models the Doppler shifted echolocation signals and has a width of $\sigma_s = 0.5$ kHz which corresponds to an average velocity of detected objects of 2 m/s. The relative amplitudes of the white noise and the gaussian distribution were chosen such that Doppler shifted echos occur three times as frequently as signals of external ultrasound sources. Figure 2 shows the resulting ultrasound spectrum.

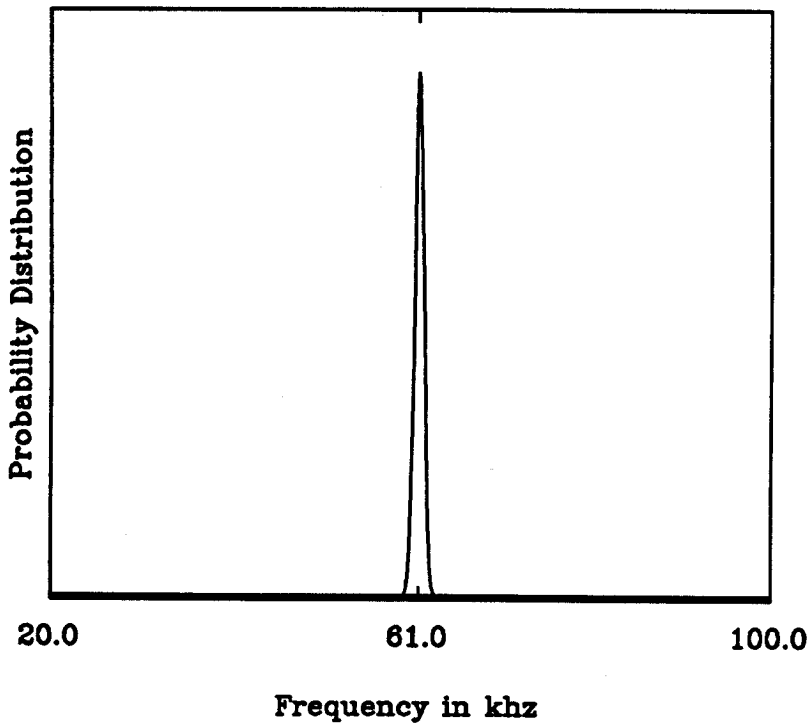

Fig.2 The probability distribution of the input signals versus the frequency of the signal, as assumed in the model. A Doppler shifted echo occures three times as frequently as a signal of external ultrasound sources.

4. The Simulation

In Fig. 1B we see, that the relevant region of the auditive cortex of *Pteronotus parnelli rubiginosus* for the resolution of the echolocation signals is very narrow along the anteroposterior axis. Thus we used for our computer simulation a narrow stripe arranged as a rectangle of 5×25 neurons with the longer side running along the anteroposterior direction.

Figure 3 shows the Kohonen net during three different phases of the learning process. Each box represents a neuron and displays the value of its best frequency. Figure 3a shows the initial state. Each neuron was assigned to a frequency drawn randomly from the range between 20 and 100 kHz. In Fig. 3b, after 500 learning steps, a continous

78	45	63	43	75
51	77	28	86	91
52	80	24	34	45
52	85	91	85	84
23	97	26	27	37
96	28	98	86	82
44	99	50	81	42
52	86	74	92	75
66	39	56	41	34
99	23	77	69	61
42	47	81	38	100
93	86	56	45	23
36	70	46	59	22
62	59	80	97	25
64	92	94	23	84
83	59	31	89	47
76	71	41	41	89
72	27	85	27	67
51	23	93	100	27
89	52	32	42	65
48	44	30	65	45
21	34	83	77	31
25	38	82	38	79
47	75	43	86	64
20	73	43	51	64

Fig.3a The initial state of the neurons with their randomly chosen best frequencies. Each neuron is represented by a box displaying the associated best frequency. The neurons are arranged as a 5 × 25-lattice.

28	28	30	32	35
28	29	31	33	36
30	31	32	35	37
33	33	35	37	39
36	37	38	39	41
40	41	41	43	44
44	44	45	46	47
48	48	49	49	50
51	52	52	52	53
54	54	55	55	55
57	57	57	57	57
58	58	58	58	58
59	59	59	59	59
60	60	60	60	60
60	60	60	60	60
60	60	60	60	60
60	60	60	60	60
60	60	60	60	60
61	61	61	61	61
62	61	61	61	61
62	62	62	62	62
63	63	63	63	62
64	64	63	63	63
64	64	64	64	63
65	64	64	64	64

Fig.3b The situation after 500 learning steps. At this stage the initial random correspondene between neurons and best frequencies has already given way to a tonotopic representation of the relevant frequency range.

36	33	29	26	25
38	35	32	30	27
40	39	37	35	33
44	42	41	39	39
47	46	44	44	44
50	49	48	48	49
54	53	53	54	54
58	58	58	58	58
59	59	59	59	59
60	60	60	60	60
60	60	60	60	60
61	61	61	61	61
61	61	61	61	61
61	61	61	61	61
61	61	61	61	61
62	62	62	62	62
62	62	62	62	63
62	62	63	63	63
64	64	64	64	65
68	68	68	69	68
72	73	73	74	73
75	77	79	81	81
78	80	84	87	88
81	83	87	91	93
82	85	90	94	96

Fig.3c The final state of the "auditive cortex" after 5000 learning steps. As a result of the narrow peak of the probability distribution of the sensory signals at 61kHz, a very disproportionate representation of the Doppler shifted echolocation signals has emerged. The associated neurons constitute almost half of the whole cortex.

relation between the frequencies as input signals and their assigned location on the net has evolved. To build up an neighbourhood conserving topology mapping between input space and neural net is one of the main features of the Kohonen model. The final state after 5000 learning steps is shown Fig. 3c. We recognize a second main feature of the model that it represents input signals corresponding to their probability of occurrence. The extreme peak of the probability density of the input signals causes an occupation of a large part of the "auditive cortex" with best frequencies from a small interval around the echolocation frequency of 61 kHz. For this simulation, the time dependency of the step size ϵ and the lateral width σ were chosen as follows: $\sigma(t) = \sigma_i[1 + exp(-(5t/t_{max})^2)]$ where $\sigma_i = 5$, $\epsilon(t) = exp(-(5t/t_{max})^2)$. t denotes the number of performed learning steps. The maximum number of learning steps t_{max} was $t_{max} = 5000$.

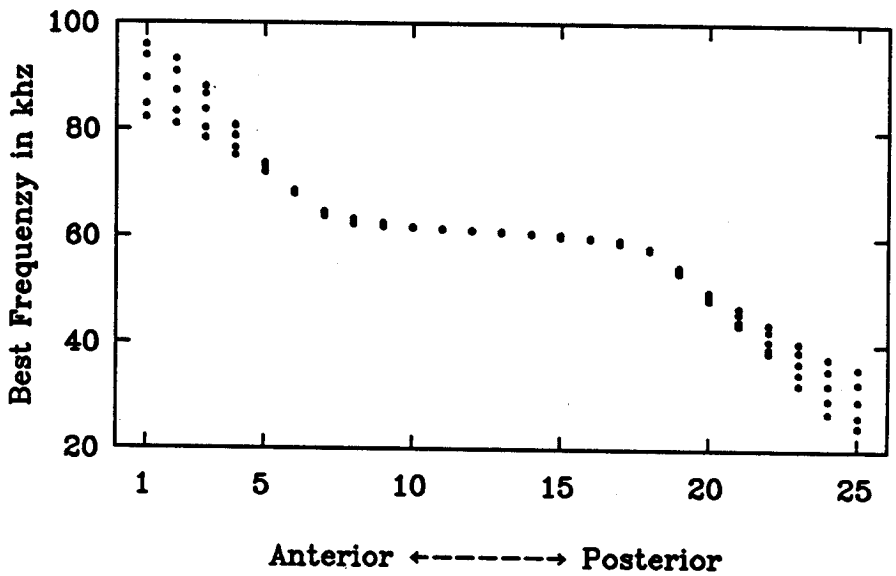

Fig.4 A representation of the results of our computer simulation analogous to the representation of the experimental data in fig. 1C. The best frequencies of all neurons are plotted versus their coordinates 1 to 25 along the anteroposterior axis of our cortex model. For each position there are five neurons, forming a row in Fig. 3.

The simulation shows that it can reproduce the qualitative features of the experimental results, namely the tonotopy of the mapping along the anteroposterior axis and the disproportionally large representation of the Doppler shifted orientation signals. The latter property can be seen more easily in Fig. 4, where we chose the same representation for our theoretical data from Fig. 3 as in Fig. 1C for the measured distribution of the best frequencies. Each neuron is described by its location 1 to 25 on the anteroposterior axis of our cortex model and its best frequency. In both diagrams, Fig. 1C and Fig. 4, the plateau region indicates that nearly half of the whole cortex is devoted to the analysis of the Doppler shifted echos. The size of this plateau is only determined by the probability distribution of the input signals.

5. An analytical Solution

With the following two assumptions the final state of Kohonen's selforganising mapping can be described mathematically.

i) We assume that for sufficiently large systems $\mathbf{w_r}$ is sufficiently slowly varying with $\mathbf{r}$ to allow replacing it by a corresponding smooth function $\mathbf{w(r)}$ over a continuum of $\mathbf{r}$-values. This basically assumes that the topological ordering of the final state has already occurred.

ii) We assume bijective equilibrium configurations. This also assumes that the input space is of same dimension as the used neural net.

For the equilibrium state of $\mathbf{w(r)}$ we get the differential equation

$$\mathbf{J} \cdot \nabla_{\mathbf{r}} \ln(P(\mathbf{w(r)}) \cdot J) = -\frac{1}{2}\Delta_{\mathbf{r}}\mathbf{w}. \tag{4}$$

with the Jacobian $J_{ij} = \frac{\partial}{\partial r_j} w_i(\mathbf{r})$ and $J = Det(\mathbf{J})$ (Ritter und Schulten 1986). In the following we are interested in the one-dimensional case, because the input space of our model, the ultrasound spectrum, is one-domensional as well. Then, equation (4) can be written as

$$\frac{d}{dr} \ln P(w(r)) = -\frac{3}{2}\frac{d}{dr} \ln\left(\frac{dw}{dr}\right). \tag{5}$$

Since $w(r)$ represents the inverse of the mapping from the input space to the neural net, the *local magnification factor* M of the mapping is given by $M = 1/J$ with $J = dr/dw$. Now we can describe the relation between local magnification factor M and signal probability distribution $P(f)$ by the simple dependency

$$M(f) = J^{-1} = \frac{dr}{dw} \propto P(f)^{2/3}. \tag{6}$$

We solve this equation for the signal spectrum of Fig. 2. This spectrum can be written as

$$P(f) = \frac{P_0}{f_2 - f_1} + (1 - P_0)\frac{1}{\sqrt{2\pi}\sigma_s} exp\left(-\frac{(f - f_e)^2}{2\sigma_s^2}\right) \quad f_1 \leq f \leq f_2 \tag{7}$$

where $\sigma_s = 0.5kHz$, $f_e = 61.0kHz$, $f_1 = 20kHz$, $f_2 = 100kHz$ and $P_0 = 1/4$. P_0 is the probability for the occurence of a stimulus of the white noise. f_1 and f_2 are the band limits of the received ultrasound spectrum.

The integral over the whole distribution is not exactly equal to unity, but the error is negligible because σ_s is small against $f_2 - f_1$. Since we have chosen $P_0 = 1/4$, Doppler shifted echolocation signals occur three times as frequent as signals of the homogenous underground noise (see Fig.2). With equation (6) we get

$$\frac{dr}{dw} = C \cdot \left(\frac{P_0}{f_2 - f_1} + (1 - P_0)\frac{1}{\sqrt{2\pi}\sigma_s} exp\left(-\frac{(f - f_e)^2}{2\sigma_s^2}\right)\right)^{2/3} \tag{8}$$

with C as integration constant. Integrating yields

$$r(w) - r_1 = C \cdot \int_{w_1}^{w} \left(\frac{P_0}{f_2 - f_1} + (1 - P_0) \frac{1}{\sqrt{2\pi}\sigma_s} exp\left(-\frac{(f - f_e)^2}{2\sigma_s^2} \right) \right)^{2/3} df. \qquad (9)$$

We solve this integral numerically and compare the calculated $w(r)$ with the $w(r)$ of a simulation.

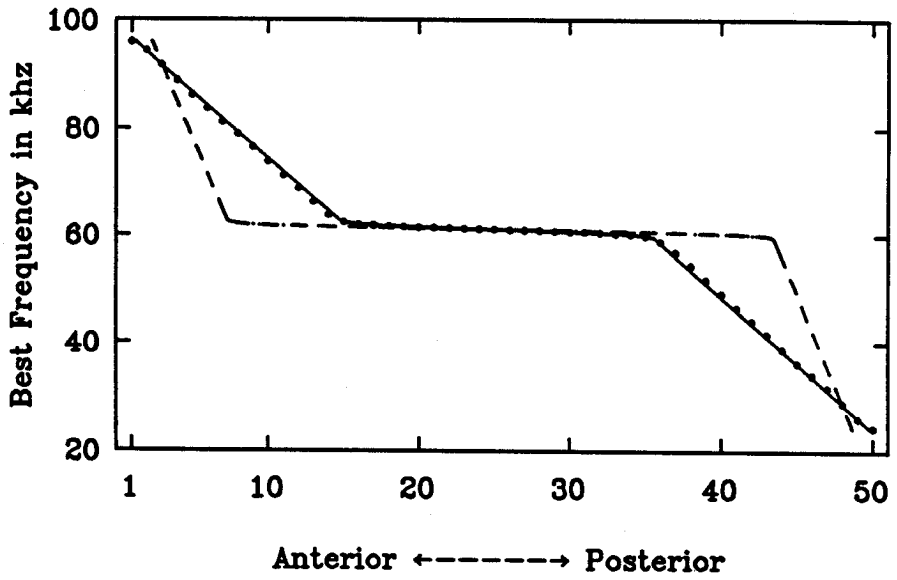

Fig.5 The solid curve represents the result of the analytical calculation. The data provided by the computer simulation are marked by points and agree very well with the theoretical curve. The dashed line shows the intuitive but incorrect expectation, namely a magnification factor proportional to the probability density of the input signals.

For this simulation we used instead of a square lattice as "auditive cortex" a chain of 50 neurons, because our analytical calculations apply only for one-dimensional nets. In view of the narrow shape of the auditory cortex this should be a justified simplification. The simulation result and the result of the analytical calculation are compared in Fig. 5, where we used again the same display format as in Fig. 2C and Fig. 4. The data points of the simulation are fitted very well by the curve of the analytical calculation. Intuitively one would expect a local magnification factor $M(f)$ proportional to the probability density $P(f)$. This would correspond to the dashed curve in Fig. 5, which, however, significantly deviates from the simulation results.

6. Conclusion

We have investigated the possibility that the highly disproportionate representation of sound frequencies in the auditory cortex of the bat *Pteronotus parnelli rubiginosus* need not be prewired initially but could instead result from adaptation of the neurons to repeated sensory experiences. Following a suggestion by Kohonen for a neurally plausible adaptation law (Kohonen 1982a, 1982c, 1984), we compared the representation generated by a computer simulation and experimental data. We found good qualitative agreement, provided that the disproportionality of the frequency representation is reflected in the statistics of the sensory experiences. For the idealization of a one-dimensional cortex, the relationship between the probability distribution of the sound frequencies and the distortion of the representation resulting from the model is calculated analytically. The results support the idea that very simple adaptation laws together with suitable signal statistics can lead to the adaptive formation of interesting sensory maps.

Acknowledgments

This work has been supported by the German Ministry for Science and Technology (ITR-8800-G9).

References

Edelman GM, Finkel LH (1985) Neuronal group selection in the cerebral cortex. In: 1st Symposium of the Neurosciences Institute, La Jolla, California, October 3-8 1982

Gerthsen, Kneser, Vogel (1986) Physik, Springer-Verlag, Heidelberg, pp 164-165

Kohonen T (1982a) Self-organized Formation of Topologically Correct Feature Maps. Biol Cybern 43:59-69

Kohonen T (1982b) Analysis of a Simple Self-organizing Process. Biol Cybern 44:135-140

Kohonen T (1982c) Clustering, Taxonomy and Topological Maps of Patterns. Proc 6th Int Conf on Pattern Recognition, Munich pp 114-128

Kohonen T (1984) Self-Organization and Associative Memory. Springer Series in Information Sciences 8, Heidelberg

Merzenich MM, Knight PL, Roth GL (1975) Journal of Neurophysiology 38:231

Ritter H, Schulten K (1986) On the Stationary State of Kohonen's Self-Organizing Sensory Mapping. Biol Cybern 54:99-106

Suga N, Jen PH (1976) Disproportionate Tonotopic Representation for Processing CF-FM Sonar Signals in the Mustache Bat Auditory Cortex. Science 194:542-544

Takeuchi A, Amari S (1979) Formation of topographic maps and columnar microstructures. Biol Cybern 35:63-72

Willshaw DJ, Malsburg C von der (1976) How patterned neural connections can be set up by self-organisation. Proc R Soc Lond Ser B 194:431-445

Willshaw DJ, Malsburg C von der (1979) A marker induction mechanism for the establishment of ordered neural mappings: its application to the retinotectal problem. Proc R Soc Lond Ser B 287:203-243

Woolsey CN, Harlow HF (1958) Biological and Biochemical Basis of Behavior. Univ. of Wisconsin Press, Madison. pp 63-81